CHEMISTRY
A EUROPEAN JOURNAL

DOI: 10.1002/chem.200601096

Pt^0 and Pd^0 Olefin Complexes of the Metalloid N-Heterocyclic Carbene Analogues $[E^I(ddp)]$ (ddp = 2-{(2,6-diisopropylphenyl)amino}-4-{(2,6-diisopropylphenyl)imino}-2-pentene; E = Al, Ga): Ligand Substitution, H−H and Si−H Bond Activation, and Cluster Formation**

Andreas Kempter, Christian Gemel, and Roland A. Fischer*[a]

Abstract: Various products of the reaction of [E(ddp)] (ddp = 2-{(2,6-diisopropylphenyl)amino}-4-{(2,6-diisopropylphenyl)imino}-2-pentene; E = Al, Ga) with Pt^0 and Pd^0 olefin complexes are reported. Thus, the reaction of $[Pt(cod)_2]$ (cod = 1,5-cyclooctadiene) with two equivalents of [Ga(ddp)] yields $[Pt(1,3\text{-}cod)\{Ga(ddp)\}_2]$ (**1**), whereas treatment of $[Pd_2(dvds)_3]$ (dvds = 1,1,3,3-tetramethyl1,3-divinyldisiloxane) with [E(ddp)] leads to the monomeric compounds [(dvds)Pd{E(ddp)}] (E = Ga (**2a**), Al (**2b**)) by substitution of the bridging dvds ligand. Both **1** and **2a** readily react with strong π-acceptor ligands such as CO or *t*BuNC to give the dimeric compounds $[M\{\mu^2\text{-}Ga(ddp)\}(L)]$ (L = CO, *t*BuNC; M = Pt (**3a**, **5a**), Pd (**3b**, **5b**)), respectively. Based on ^1H NMR spectroscopic data, $[Pt\{Ga(ddp)\}_2(CO)]$ is likely to be an intermediate in the formation of **3a**. Furthermore, reactions of **1** with H_2 and $HSiEt_3$ yield the monomeric compounds $[Pt\{Ga(ddp)\}_2(H)_2]$ (**7**) and $[Pt\{Ga(ddp)\}_2(H)(SiEt_3)]$ (**8**). Finally, the reaction of $[Pt(cod)_2]$ with one equivalent of [Ga(ddp)] in the presence of H_2 in hexane gives the new dimeric cluster $[Pt\{\mu^2\text{-}Ga(ddp)\}(H)_2]_2$ (**9**).

Keywords: carbene ligands · Group 13 elements · oxidative addition · palladium · platinum

Introduction

The coordination chemistry of the heavier Group-14 carbene and carbyne ligand analogues with transition metals has attracted unbroken interest since their discovery by Fischer and Maasböl in 1963,[1] with the molybdenum plumbylidine complex discovered by Filippou et al. being a typical and more recent example.[2] Likewise, the use of N-heterocyclic carbenes (NHCs) as versatile ancillary ligands in homogeneous organometallic catalysis[3] had a strong influence on the advent and rise of the chemistry of related Group-13 element heterocycles.[4] The neutral six-membered β-diketiminato complexes $[{:}E\{[N(Ar)C(Me_2)]_2CH\}]$ (Ar = $C_6H_3iPr_2$-2,6; E = Al,[5] Ga,[6] In,[7] Tl[8]), the anionic five-membered diazabutadienido complexes $[Ga\{N(R)C(H)\}_2]^-$ (R = *t*Bu, Ar),[9] and, very recently, the neutral four-membered guanidinate complexes $[E\{(Ar)NC(NCy_2)N(Ar)\}]$ (E = Ga, In, Tl)[10] have been described during the last five years. Studies at the DFT level of theory have revealed common properties of these Group-13 element heterocycles, particularly the existence of a directional lone-pair of sp character at the Group-13 atom. Likewise, the overlap between the N p orbitals and the p_z orbital at the Group 13 center is almost negligible, the E−N bonds exhibit a high ionic character, and the energetic gaps between the metal lone-pair (sp) and the free metal p orbitals orthogonal to the heterocyclic plane are quite large (ca. 100 $kcal\,mol^{-1}$).[4] Altogether, these properties suggest that these compounds should behave as strong σ-donors while being rather weak π-acceptors, in analogy to NHCs. Indeed, the first examples of transition-metal complexes have been reported, including $[\{(ddp)Ga\}Fe(CO)_4]$ by Power et al.,[11] and [{(ddp)Ga}Au{GaCl(ddp)}],[12] $[(Ph_3P)_2Rh\{Ga(ddp)\}(\mu\text{-}Cl)]$,[13] or $[\mu^2\text{-}\{Al(ddp)\}\{Pd(dvds)\}_2]$[14] (dvds = 1,1,3,3-tetramethyl-1,3-divinyldisiloxane) by our group. Compared to these few cases, the related co-

---

[a] A. Kempter, Dr. C. Gemel, Prof. Dr. R. A. Fischer
Anorganische Chemie II – Organometallics & Materials
Ruhr-Universität Bochum, 44780 Bochum (Germany)
Fax (+49) 234-321-4174
E-mail: roland.fischer@ruhr-uni-bochum.de

[**] Organo Group 13 Complexes of Transition Metals XLVI; for part XLV see: B. Buchin, C. Gemel, A. Kempter, T. Cadenbach, R. A. Fischer, *Inorg. Chim. Acta* **2006**, 359, 4833–4839

Supporting Information for this article is available on the WWW under http://www.chemeurj.org/ or from the author.

ordination chemistry of the Group-13 element diyls :ECp* (E = Al, Ga, In) is rather well developed, with some emphasis on homoleptic $[M_a(ER)_b]$ complexes and clusters.[15] However, all the above-cited studies have largely concentrated on synthetic, structural, and bonding issues, and not much is known about the reactivity of the metal centers supported by these quite exotic metalloid ligands. C–H activation of benzene and oxidative addition of $HSiEt_3$ takes place at the unsaturated intermediate $[Ni(AlCp^*)_3]$[16] and related multiple C–H activation reactions at the methyl groups of the Cp* moiety possibly limit the accessibility of $[M(AlCp^*)_5]$ (M = Fe, Ru).[17] The reaction of $[RhCp^*(L)(CH_3)_2]$ with [GaCp*] to yield the zwitterionic rhodenocenium species $[RhCp^*(C_5Me_4GaMe_3)]$ involves several steps of substitution and rearrangement together with an unusual C–C bond rupture, which has been mechanistically studied.[18,19] In summary, the stabilization of unsaturated and very electron-rich transition-metal centers as well as the synthesis of novel bimetallic M/E cluster compounds with varying M:E ratios depending on the steric demand of the :ER diyl ligands seem attractive goals in this context. Using the bulkier $[Ga(C_5Me_4Ph)]$ rather than [GaCp*] does, in fact, lead to clusters with an increased M:Ga ratio when treated with d^{10} metal sources.[20] Obviously, the Group-13 element heterocycles offer complementary degrees of freedom by combining high steric shielding with strong σ-donor properties. Herein we wish to report on the synthesis and characterization of Pt^0 and Pd^0 olefin complexes of [Ga(ddp)] and [Al(ddp)], their structural properties, as well as reactivity studies involving olefin substitution, hydrogenation, and H_2 and Si–H bond-activation reactions.

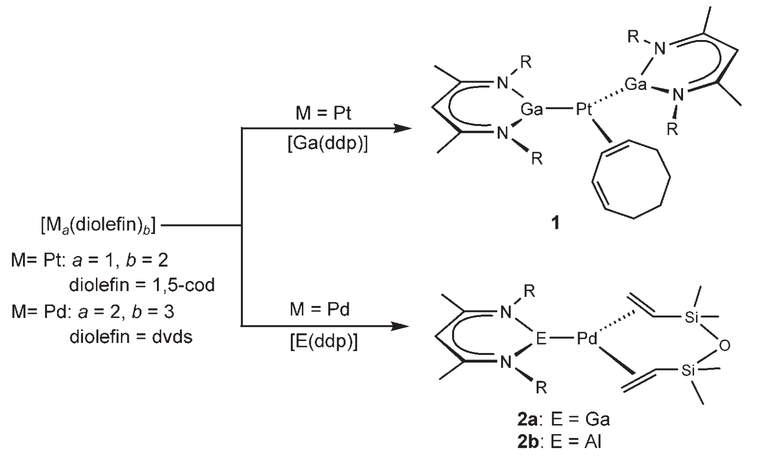

Scheme 1. Synthesis of $[(1,3\text{-cod})Pt\{Ga(ddp)\}_2]$ (**1**) and $[(dvds)Pd\{Ga(ddp)\}]$ (**2a,b**).

Results

Reactions of $[Pt(cod)_2]$ and $[Pd_2(dvds)_3]$ with [E(ddp)]: The entry into the chemistry of potentially reactive, coordinatively unsaturated $[M\{E(ddp)\}_n]$ complexes or intermediate fragments is based on the substitution of labile olefin ligands. The more strongly bound CO ligands of carbonylmetal fragments $[L(CO)_nM]$ cannot be fully displaced,[15] and the presence of alkyl or halide groups at transition metal centers in a medium or higher oxidation state may create a problem due to the strongly reducing power of the Group-13 element species, for example leading to the insertion of the E^I center into M–C, M–H, or M–X bonds (X = halide, etc.).[12,13,21–23] Side reactions of the displaced olefin ligand with the Group-13 metalloid ligand must also be taken into account and need to be avoided by choosing suitable reaction conditions. For example, [AlCp*] reacts with dvds to yield the compound $[(dvds)(\mu^2\text{-}Cp^*Al)_2]$, which can be described as a double adduct of [Cp*Al] with the two C=C double bonds of the dvds ligand. The resulting compound has an adamantyl-like structure and emphasizes the carbenoid character of these kind of ligands.[24] Upon treatment of $[Pt(cod)_2]$ with [Ga(ddp)] at room temperature in n-hexane (Scheme 1), only one cod ligand is substituted to give the monomeric complex $[(1,3\text{-cod})Pt\{Ga(ddp)\}_2]$ (**1**). The remaining coordinated cod ligand is isomerized to the thermodynamically more stable 1,3-cod. We have not elucidated the mechanistic details of this rearrangement but suggest that the situation should be similar to the classical catalytic olefin isomerization processes with an η^3-allyl hydride complex as an intermediate.[25] Compound **1** decomposes in solution as well as in the solid state upon contact with air, but is stable under an inert atmosphere up to 170 °C.

The ^1H NMR spectrum of **1** at room temperature consists of several broad, partially overlapping signals in the expected regions for a ddp and a η^2-coordinated 1,3-cod ligand. With the exception of the γ-carbon of the ddp backbone, which gives rise to a sharp singlet at $\delta = 4.99$ ppm that is used as a diagnostic tool in this chemistry, none of the resonances can be unequivocally assigned without employing more sophisticated NMR techniques. However, the ^1H NMR spectrum is reproducible and characteristic. The NMR spectrum of **1** is given as Supporting Information. It should be noted that the spectra recorded at both low and high temperature were also unassignable.

The ^{13}C NMR spectrum is also not fully assignable. Two signals for the C=N carbon atoms appear at $\delta = 166.1$ and 164.6 ppm, and only one signal for the γ-carbon atoms of both ddp moieties is found at $\delta = 100.0$ ppm. Since at this stage of our exploration we are not focusing on mechanistic studies or a detailed characterization of the solution properties of the compounds, the rigorous assignment of these complex NMR spectra appeared unnecessary. We instead used X-ray single-crystal structure analysis as the tool of choice to elucidate the molecular structure of the compounds in the solid state and employed elemental analysis and the NMR fingerprint to verify the purity and homogeneity of the new compounds.

Similarly to the synthesis of the PtGa$_2$ compound **1**, the PdE compounds [(dvds)Pd{E(ddp)}] (**2a**: E = Ga; **2b**: E = Al) were obtained in yields of around 90 % by treatment of [Pd$_2$(dvds)$_3$] with [E(ddp)] (E = Al, Ga) in hexane at room temperature (Scheme 1). Compound **2a** forms bright yellow, rhombohedral crystals upon slow crystallization from hexane at 4 °C and rapidly decomposes on contact with air or moisture as well as on heating to temperatures above 200 °C in the solid state. The ^{1}H NMR spectrum of **2a** at room temperature shows one typical set of signals for a C_s-symmetric, coordinated [Ga(ddp)] moiety. Two distinct signals for the SiMe$_2$ groups can be observed at $\delta = 0.45$ and -0.16 ppm. As we have communicated recently,[14] the reaction of [Pd$_2$(dvds)$_3$] with [Al(ddp)] gives the interesting dimer [{Pd(dvds)}$_2${μ^2-Al(ddp)}], which contains a Pd$_2$Al core, and the monomeric complex [(dvds)Pd{Al(ddp)}] (**2b**) in high yields, depending on the ratio of the starting materials. Thus, an excess of [Al(ddp)] (> 2.5 equiv) is required to quantitatively transform the dimeric intermediate into the monomer **2b**. Evidently, a monomer–dimer equilibrium occurs in solution. The ^{1}H and ^{13}C NMR spectra of **2b** are very similar to those of **2a**, and these will not be discussed here in detail.

Molecular structures of [(1,3-cod)Pt{Ga(ddp)}$_2$] (1) and [(dvds)Pd{E(ddp)}] (2a,b): Deep red, octahedral crystals of **1** suitable for X-ray analysis were obtained by recrystallization of the crude product from benzene. It crystallizes in the orthorhombic space group $P2_12_12_1$. The molecular structure of **1** in the solid state is depicted in Figure 1. The trigonal-planar 16 VE Pt^0 center is surrounded by two [Ga(ddp)] moieties and one η^2-coordinated 1,3-cod ligand. The Pt–Ga distances are almost equal (Pt–Ga(1) 2.342(1), Pt–Ga(2) 2.346(1) Å). These bonds are quite similar in length and only slightly longer than the Pt–Ga distances in the homoleptic complex [Pt(GaCp*)$_4$] (2.335(2) Å) or the terminal Pt–Ga distances in the dimeric cluster [Pt$_2$(GaCp*)$_5$] (2.326(2) and 2.331(1) Å). The N-heterocyclic ligand expectedly exerts only a marginal effect on the Pt–Ga bond distance, thus showing the absence of particular steric constraints or crystal packing effects. The Ga–N bond lengths vary in the range 2.001(8) to 2.024(8) Å, which is only slightly shorter than in free [Ga(ddp)] (av 2.054 Å). This property parallels the well-documented shrinkage of the E–Cp* distance (element atom to the centroid of the η^5-Cp* ligand) in the related complexes [L$_n$M–ECp*] as a consequence of the increased electrophilic character of E^I upon coordination. Consistently, a similar shrinkage of the Ga–N bond length of coordinated [Ga(ddp)] is found in the complexes [(Ph$_3$P)$_2$Rh{Ga(ddp)}(μ-Cl)] (1.992–1.996 Å) and [(coe)(benzene)Rh{(ddp)GaCl}] (1.97–2.012 Å).[13]

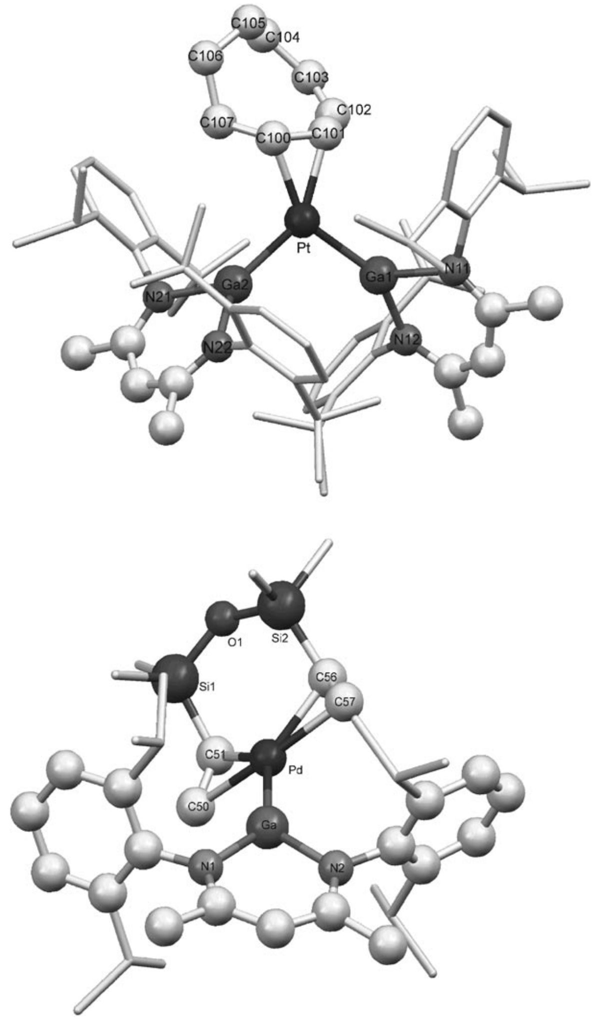

Figure 1. Mercury plot of **1** (top) and **2a** (bottom). Hydrogen atoms have been omitted for clarity. Selected bond lengths [Å] and angles [°] for **1**: Pt–C100 2.118(8), Pt–C101 2.155(8), Pt–Ga1 2.346(1), Pt–Ga2 2.342(1), Ga1–N11 2.017(6), Ga1–N12 1.994(6), Ga2–N1 2.008(7), Ga2–N2 2.020(5), C100–C101 1.449(11), C102–C103 1.305(14); Ga2-Pt-Ga1 105.49(4), N11-Ga1-N12 90.5(2), N21-Ga2-N22 91.5(2), C1-Pt-C8 39.6(3). Selected bond lengths [Å] and angles [°] for **2a**: Pd–Ga 2.3962(6), Pd–C50 2.167(4), Pd–C51 2.175(4), Pd–C56 2.189(4), Pd–C57 2.162(4), Ga–N1 1.997(3), Ga–N2 1.990(3), C50–C51 1.389(6), C56–C57 1.402(6); N1-Ga-N2 90.82(12), N1-Ga-Pd 137.83(9), N2-Ga-Pd 131.35(9). The isostructural Al congener **2b** has been communicated earlier.[14] Selected bond lengths [Å] and angles [°] for **2b**: Pd1–Al 2.3702(10), Pd1–C50 2.142(3), Pd1–C51 2.173(3), Pd1–C56 2.173(3), Pd1–C57 2.146(3), Al–N1 1.906(3), Al–N2 1.912(3), C50–C51 1.405(4), C56–C57 1.412(4); N1-Al-N2 92.00(11), N1-Al-Pd1 130.46(9), N2-Al-Pd1 137.54(9).

The bond lengths for the cod double bonds in **1** are 1.449(11) Å for the uncoordinated and 1.30(2) Å for the coordinated one. This bond length for the coordinated C=C double bond in **1** is substantially shorter than in the related complex [Pd(dcpe)(η^2-1,3-butadiene)] (1.323 and 1.405 Å; dcpe = bis(dicyclohexyl)phosphanylethane),[26] which shows the somewhat stronger π-backbonding character of the metal–olefin bond.

Complex **2a** crystallizes in the triclinic space group $P\bar{1}$. Its molecular structure (Figure 1) exhibits a coplanar arrangement of the vinyl groups of the dvds ligand and the Pd and Ga atoms (angular sum: $C{=}C_{cent}$, Pd, Ga: 358.92°). The Pd–C distances (2.17–2.19 Å) are very similar to the respective distances in $[(Me_3P)Pd(\eta^2,\eta^2\text{-diallyl ether})]$ (2.15–2.16 Å),[27] whereas the C=C bond lengths are considerably longer (1.404(7) and 1.391(7) Å in **2a** versus 1.364 and 1.387 Å in $[(Me_3P)Pd(\eta^2,\eta^2\text{-diallyl ether})]$), which points to a distinctly higher degree of π-backbonding to the olefins in the [Ga(ddp)] complex than in its phosphane analogue. Interestingly, the monomeric NHC complex [(NHC)Pd(dvds)] (NHC = $(2,6\text{-diisopropylphenyl-N})_2C_3H_2$) shows very similar C=C bond lengths (1.40 Å) to those in **2a**. Thus, the σ-donor properties of [Ga(ddp)] indeed seem to be more like those of NHCs rather than electron-rich phosphanes. The same is true for [Al(ddp)] (see below). The Pd–Ga distance (2.396(1) Å) is slightly longer than in the monomeric compound $[Pd(GaCp^*)_4]$ (2.37 Å), but expectedly shorter than the terminal Pd–Ga distances in the trimetallic compound $[Pd_3(GaCp^*)_8]$ (2.40–2.45 Å).[28] The Ga–N distances in **2a** (1.997(3) and 1.990(3) Å) are very similar to those in **1** and are shorter than in the free ligand (vide supra).

Crystals of **2b** suitable for X-ray analysis were obtained by cooling a saturated solution in hexane to −30 °C overnight. Complex **2b** is essentially isostructural with **2a**, with only slight deviations. The Pd–Al distance (2.37 Å) is slightly longer than in $[Pd_2(AlCp^*)_5]$ (terminal Pd–Al: 2.32 Å) but similar to the terminal Pd–Al bond lengths found in the trinuclear cluster $[Pd_3(AlCp^*)_2(\mu^2\text{-}AlCp^*)_2(\mu^3\text{-}AlCp^*)_2]$ (2.38 and 2.35 Å).[28] Both C=C distances (1.412 and 1.409 Å) are similar to those found in **2a** and thus to those in its NHC analogue, which indicates the similarly strong σ-donor capabilities of [Al(ddp)] and [Ga(ddp)] (vide supra).

Substitution of the coordinated olefins in 1 and 2a: The reaction of **1** with an excess of CO in toluene gave bright yellow crystals of $[\{Pt(CO)[\mu^2\text{-}Ga(ddp)]\}_2]$ (**3a**) (Scheme 2). Surprisingly, **3a** is insoluble in all common organic solvents, thus preventing the recording of solution NMR spectra. All attempts to record solid-state NMR spectra gave only broad, overlapping, and hence uninterpretable, signals. However, when the reaction mixture was not stirred during the synthesis of **3a**, single crystals suitable for X-ray analysis (see below) crystallized directly from solution.

The IR spectrum of **3a** reveals two sharp absorptions at 1936 and 1993 cm^{-1} in the region typical for terminal CO ligands. These IR absorptions are at significantly higher wavenumbers than those of the saturated PPh_3 complex $[Pt(PPh_3)_3(CO)]$ (1903 cm^{-1})[29] but comparable to $[Pt_2(CO)_2(\mu^2\text{-}GaCp^*)_3]$ (1962 cm^{-1}).[28]

On addition of exactly one equivalent of CO to **1** in C_6D_6, an intermediate species can be observed by ^1H NMR spectroscopy. Thus, besides the signals for free 1,3-cod, one new set of signals for a coordinated [Ga(ddp)] is observed. A sharp singlet at $\delta = 4.94$ ppm (2H) can be assigned to the γ-CH proton of the ddp backbone. The isopropyl groups of the ddp ligand give rise to one septet at $\delta = 3.09$ ppm (8H) as well as two doublets ($\delta = 1.23$ and 1.14 ppm, 24H each). The CH_3 groups attached to the metallacycle give rise to a singlet at $\delta = 1.51$ ppm (12H). The lack of signals for free [Ga(ddp)] suggests that both ligands are still coordinated to the Pt center. A fast exchange of coordinated and free [Ga(ddp)] in solution cannot be excluded, yet the rather large high-field shift of the γ-CH proton signal ($\delta = 4.94$ ppm) points to a coordination of both [Ga(ddp)] ligands. Thus, $[\{(ddp)Ga\}_2Pt(CO)]$ (**4**; Scheme 2) is a reasonable suggestion for the structure of this intermediate, that is, the direct substitution product of 1,3-cod with CO in **1**.

Similarly to the preparation of **3a**, the reaction of **2a** with CO gives $[Pd\{\mu^2\text{-}Ga(ddp)\}CO]_2$ (**3b**). Its molecular structure (Figure 2) is very similar to that of **3a**, with only minor deviations. However, **3b** is well soluble in organic solvents, thus allowing the recording of solution NMR spectra. All spectra are in accordance with the solid-state structure and will therefore not be discussed here in detail. The IR spectrum of **3b** reveals a sharp absorption at 1963 cm^{-1}, thus indicating the terminal coordination of CO.

As expected, the olefins can also be substituted by isonitrile ligands. The dimeric compound $[Pt\{\mu^2\text{-}Ga(ddp)\}(t\text{BuNC})]_2$ (**5a**) is formed on reaction of **1** with *t*BuNC and could be isolated as deep red crystals in high yields according to Scheme 2. Like **3a**, compound **5a** is insoluble in all common organic solvents and thus no solution NMR spectroscopic data are available. The molecular structure of **5a** was confirmed by X-ray diffraction and is discussed below, the crystals being obtained by slow diffusion of *t*BuNC into a solution of **1** in hexane or thf. When

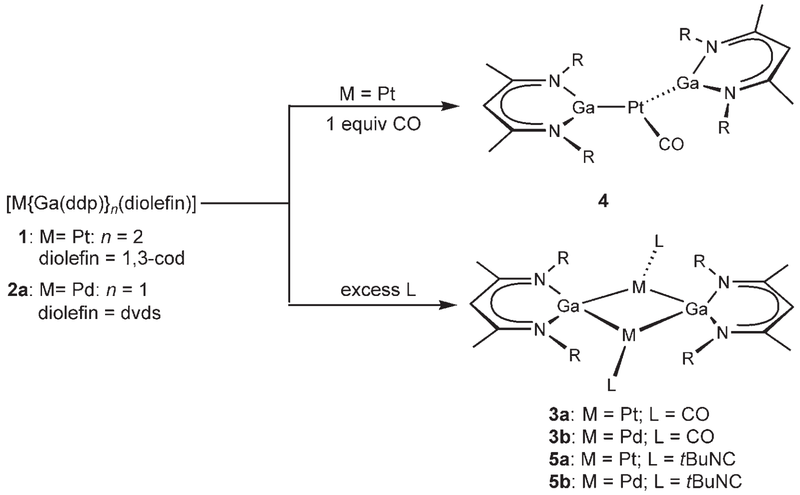

Scheme 2. Olefin substitution by CO and *t*BuNC in complexes **1** and **2a**.

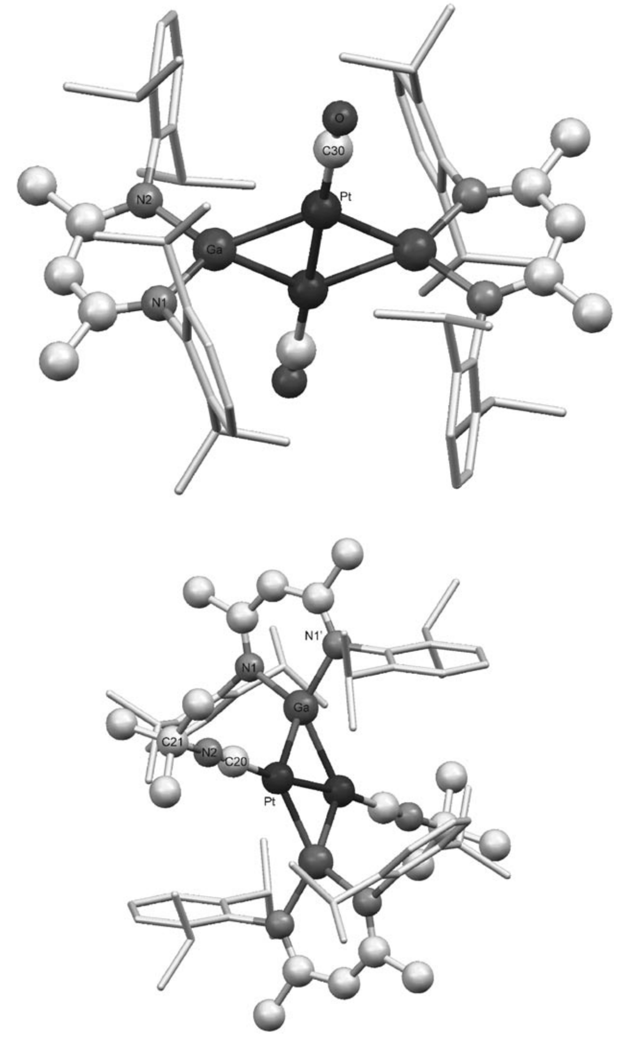

Figure 2. Mercury plot of **3a** (top) and **5a** (bottom). Hydrogen atoms have been omitted for clarity. Selected bond lengths [Å] and angles [°] for **3a**: Pt–Ga 2.4871(10), Pt–Ga* 2.5207(10), Pt–Pt* 2.6131(10), Ga–N1 1.952(6), Ga–N2 1.948(6), Pt–C30 1.947(12), C30–O 0.923(13); Ga-Pt-Ga* 117.10(3), Pt-Ga-Pt* 62.90(3), N1-Ga-N2 93.8(2), Pt-C30-O 176.7(12). * = symmetry code: $-x$, $-y+1$, $-z$. The isostructural Pd congener **3b** is shown in the Supporting Information. Selected bond lengths [Å] and angles [°] for **3b**: Pd–Ga 2.4875(7), Pd–Ga* 2.5091(7), Pd–Pd* 2.6227(12), Ga–N1 1.980(3), Ga–N2 1.971(3), Pd–C30 1.882(5), C30–O1 1.128(5); Ga-Pd-Ga* 116.68(3), Pd-Ga-Pd* 63.32(3), N1-Ga-N2 92.13(11), Pd-C30-O1 178.8(4). * = symmetry code: $-x+1$, $-y+1$, $-z$. Selected bond lengths [Å] and angles [°] for **5a**: Pt–Ga 2.4464(11), Pt–Ga* 2.4741(12), Pt–Pt* 2.6342(8), Ga–N1 1.995(4), Ga–N1* 1.995(4), Pt–C20 1.902(7), C20–N2 1.079(9); N1-Ga-N1* 92.4(2), N1-Ga-Pt 123.22(11), N1-Ga-Pt* 128.04(10), Ga-Pt-Ga* 115.27(3), Pt-Ga-Pt 64.73(3), C20-Pt-Pt* 174.1(2), Pt-C20-N2 179.3(8). * = symmetry codes: $-x+4$, $-y+1$, $-z+3$ and x, $-y+1$, z. The isostructural Pd congener **5b** is shown in the Supporting Information. Selected bond lengths [Å] and angles [°] for **5b**: Pd–Ga 2.469(2), Pd–Ga* 2.484(2), Pd–Pd* 2.6628(16), Ga–N1 2.022(3), Pd–C16 1.953(5), C16–N2 1.162(6); N1-Ga-N1* 91.02(16), N1-Ga-Pd 122.76(9), N1-Ga-Pd* 129.20(8), Ga-Pd-Ga* 114.97(7), Pd-Ga-Pd 65.03(7), C16-Pd-Pd 174.02(16), Pd-C16-N2 179.3(5). * = symmetry codes: $-x+1$, $-y+1$, $-z$ and x, $-y+1$, z.

the reaction of **1** and *t*BuNC was monitored by ^{1}H NMR spectroscopy in solution, the formation of [(ddp)Ga(*t*Bu)(CN)] (**6**) as a side product was observed. Evidently, [Ga(ddp)] is liberated in the course of the reaction and this readily reacts with *t*BuNC to give the oxidative addition product **6**. [Ga(ddp)] reacts with *t*BuNC to give **6** by insertion of the gallium diyl into $(CH_3)_3NC$ also in the absence of any platinum-containing compound. All experimental details of the preparation of **6**, spectroscopic data, and a depiction of the solid-state structure are provided as Supporting Information.

Molecular structures of 3a, 3b, 5a, and 5b: Compound **3a** crystallizes in the monoclinic space group $P2_1/n$ with half of the dimeric complex in the asymmetric unit. The molecular structure shows the [Ga(ddp)] ligands in a bridging position between the two Pt centers with slightly different Pt–Ga bond lengths (2.487(1) and 2.521(1) Å), which results in a slightly distorted square-planar arrangement of the Pt_2Ga_2 core (angular sum: 360.0°). Complex **3a** has a nearly perfectly linear arrangement of the Pt centers and the carbonyl ligands (Pt-C-O 177.29°; Pt-Pt-C 178.15°), which means that the carbonyls share a plane with the Pt and Ga centers. The Pt–Ga distances as well as the Pt–Pt distance (2.614(1) Å) in **3a** are longer than those found in the dimeric cluster [Pt_2-$(GaCp^*)_5$] (Pt–Ga around 2.46 Å; Pt–Pt: 2.582 Å), which is presumably a result of the increased steric bulk of [Ga(ddp)] with respect to [GaCp*]. The Ga–N bond lengths (average value: 1.953 Å) are significantly shorter than in **1**, which is probably caused by an acidification of the Ga centers on coordination of the [Ga(ddp)] ligand in a bridging position. The presence of the strong π-acceptor ligand CO may have an additional influence. The molecular structure of **3b** is very similar, with only slight deviations, and will therefore not be discussed here in detail.

Complex **5a** crystallizes in the monoclinic space group $C2/m$. The molecular structure is similar to that found for the carbonyl compound **3a**, with two Pt centers bridged by two [Ga(ddp)] ligands with an almost ideal square-planar arrangement (angular sum: 360.0°). The Pt–Ga distances are almost equal (Pt1–Ga1 2.446, Pt1*–Ga1 2.474 Å) and slightly shorter than in **3a**, whereas the Ga–N bond length is somewhat longer (1.995 vs. 1.953 Å in **3a**). The Pt–C distance is shorter (1.897 Å) than in **3a** (1.968 Å), but comparable to the ones in other Pt–isonitrile complexes (e.g. in [Pt_3(*t*BuNC)$_3$(μ^2-*t*BuNC)$_3$]:[30] 1.88–1.92 Å). The CN bond length (1.078 Å) is rather short, which points to a low degree of π-backbonding in **5a** caused by the bridging mode of the 2e-donor [Ga(ddp)] ligands. [Pd{μ^2-Ga(ddp)}-(*t*BuNC)]$_2$ (**5b**) is obtained similarly by reaction of **2a** with *t*BuNC (Scheme 2). The molecular structure of **5b** is very similar to that of **5a** and will therefore be not discussed here in further detail.

Oxidative addition of H_2 and $HSiEt_3$ to compound 1 and H/D exchange with C_6D_6: In contrast to **2a**, which proved to be completely inert towards H_2 and $HSiEt_3$ under various conditions, **1** was found to react readily with both reagents under ambient conditions. Thus, treatment of **1** with an excess of H_2 in hexane leads to the formation of the dihydride complex *trans*-$[Pt\{Ga(ddp)\}_2(H)_2]$ (**7**; Scheme 3). As shown by ^1H NMR spectroscopy, the diolefin ligand is completely hydrogenated in the course of the reaction. Even addition of an excess of 1,5-cod leads to a complete, and therefore obviously catalytic, hydrogenation of the ligand. Compound **7** was characterized by means of NMR spectroscopy, elemental analysis, and single crystal X-ray analysis. The ^1H NMR spectrum of **7** shows only one set of signals for the [Ga(ddp)] moieties, with one singlet at $\delta = 5.07$ ppm (2H), one septet at $\delta = 3.06$ ppm (8H), and two doublets at $\delta = 1.17$ and 1.13 ppm for the isopropyl methyl groups (each 24H). The Pt-bound H gives rise to one characteristic signal at $\delta = -4.50$ ppm, with the expected Pt satellites (2H; $J_{Pt,H} = 334$ Hz). The existence of only one set of signals for the coordinated [Ga(ddp)] moieties as well as the hydride-to-ligand ratio of 1:1 suggests the formation of a C_{2v}-symmetric Pt complex, that is, a *trans*-PtL_2H_2 structure.

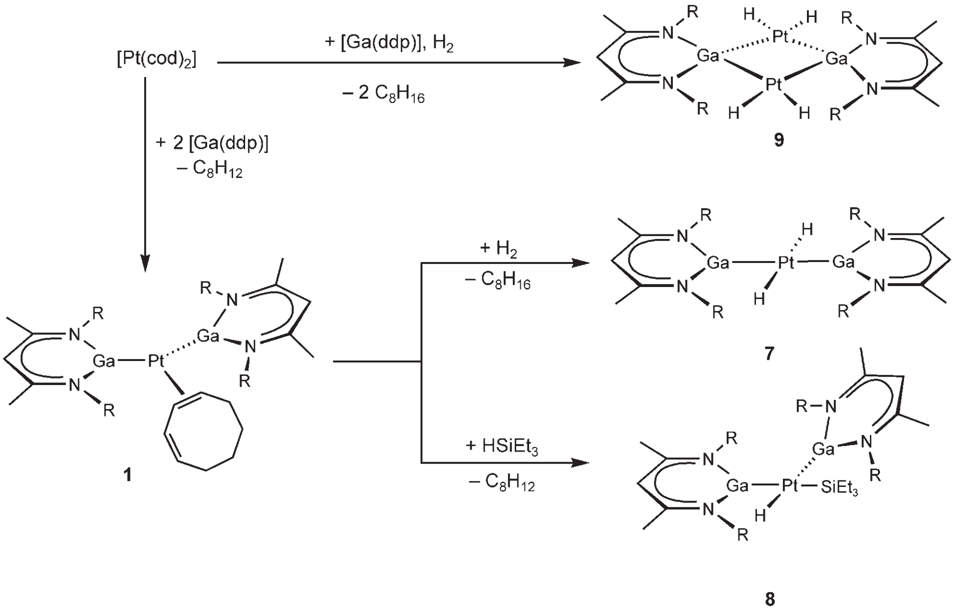

Scheme 3. Oxidative addition of H_2 and $HSiEt_3$ to **1** and hydrogenation of a 1:1 mixture of $[Pt(cod)_2]$ and [Ga(ddp)].

Monitoring the reaction in situ by ^1H NMR spectroscopy revealed the formation of an intermediate. Thus, besides **7**, a second Pt hydride species can be detected ($\delta = -3.87$ ppm, 2H; $J_{Pt,H} = 377$ Hz), which shows the same hydrogen-to-ligand ratio of 1:1 but has lower idealized symmetry (C_s) than **7**. A reasonable suggestion for the structure of this compound is a *cis*-dihydride, which is the direct product of the oxidative addition of H_2 to the unsaturated $[Pt\{(Ga(ddp)\}_2]$ fragment. The general stability of $[Pt\{(Ga(ddp)\}_2X_2]$ complexes with a *cis* arrangement of the [Ga(ddp)] ligands is shown in the formation of the *cis*-silane complex **8** (vide infra), although neither pure samples of this *cis*-dihydride complex nor crystals suitable for X-ray analysis could be obtained.

In the hydrogenation reaction of **1**, both [Ga(ddp)] ligands remain coordinated to the platinum center to form the *trans* dihydride complex **7** as the thermodynamically most stable product. But what about hydride complexes having only one [Ga(ddp)] ligand coordinated to the platinum center, in accordance with the substitution products **3a** and **5a**? Since a diolefin complex with only one Ga(ddp) ligand similar to **2a** is still unknown for platinum, a 1:1 mixture of $[Pt(cod)_2]$ and [Ga(ddp)] in thf was treated with hydrogen (1 atm) in situ. After stirring the deep-red reaction mixture for six hours at room temperature, a yellow precipitate of $[\{Pt[\mu^2\text{-}Ga(ddp)](H)_2\}_2]$ (**9**) formed (Scheme 3). The ^1H NMR spectrum of **9** shows only one set of signals for a C_{2v}-symmetric [Ga(ddp)] ligand as well as a broad signal at $\delta = -4.06$ ppm (4H), thus indicating the presence of two hydrides and one Ga(ddp) moiety coordinated to each Pt center. The ^{13}C NMR spectrum is in good agreement with this, with signals for a [Ga(ddp)] moiety with local C_{2v} symmetry.

Treatment of a red solution of **1** in hexane with an excess of $HSiEt_3$ at room temperature caused the color of the solution to immediately change to orange. After the solution had been stirred for two hours at room temperature, $[Pt\{Ga(ddp)\}_2(H)(SiEt_3)]$ (**8**) was obtained as an orange solid by precipitation at −30 °C overnight (Scheme 3). Its ^1H NMR spectrum at room temperature in C_6D_6 consists of a complex set of partially overlapping and broad signals. Whereas both γ-carbons of the heterocycles give rise to only one sharp singlet at $\delta = 4.95$ ppm, all other ddp signals are separated, thus indicating two chemically inequivalent, locally C_s-symmetric [Ga(ddp)] ligands. However, most of the signals are distinctly broadened, which indicates some kind of fluxional process in solution. The protons of the coordinated $SiEt_3$ are found at $\delta = 1.19$ (q, 6H) and 0.93 ppm (t, 9H). The hydride gives rise to a sharp triplet at $\delta = -5.63$ ppm ($J_{Pt,H} = 530$ Hz). At 70 °C, the ^1H NMR spectrum simplifies noticeably, showing only one set of signals for the ddp ligands (C_{2v} symmetry). Either reductive elimination/oxidative addition of $HSiEt_3$ or dissociation/association of [Ga(ddp)] is most likely the origin of this fluxional process, although the exact mechanism is unclear. The catalytic deuteration of $HSiEt_3$ by C_6D_6 (vide infra), however, points to the reversibility of the silane addition. Unfortunately, neither ^{29}Si nor ^{195}Pt NMR spectroscopy gave spectra with reasonable intensities, although the

^{13}C NMR spectrum of **8** is consistent with this fluxional process.

Interestingly, the hydride signal disappears on heating the NMR sample for a long period of time. Obviously an H/D exchange with the solvent C_6D_6 is taking place, which is also indicated by a concomitant increase of the solvent signal in the ^{1}H NMR spectrum. Indeed, the H/D exchange reaction is catalytic. Thus, heating a solution of **8** in C_6D_6 in the presence of a large excess of $HSiEt_3$ (about 10 equiv) leads to complete disappearance of the SiH signal in the ^{1}H NMR spectrum after two days at 70 °C, while all other signals (including those of complex **8**) remain unchanged. Again, the exact mechanism is unclear. However, taking into account that C–H activation reactions of C_6H_6 with Pt^{II} complexes are well known,[31] a C–D activation of C_6D_6 by **8** formation of a Pt^{IV} "hydride deuteride" intermediate, followed by reductive elimination of C_6D_5H and $DSiEt_3$, is a reasonable pathway.

Molecular structures of 7, 8, and 9: On recrystallization of the crude product **7** from hexane, yellow, rhombohedral crystals suitable for X-ray analysis were collected. Compound **7** crystallizes in the orthorhombic space group *C*2/*c*. The molecular structure (Figure 3) consists of a central Pt atom that is linearly coordinated by two [Ga(ddp)] moieties (Ga–Pt–Ga 180°). The Pt–Ga distances (2.304 Å) are, to the best of our knowledge, the shortest bond distances for a terminally coordinated Ga^I ligand reported so far and are considerably shorter than in **1** (2.34 Å). The presumably strong Pt–Ga interaction is also reflected by Ga–N distances of 1.96 and 1.94 Å, which are significantly shorter than in free [Ga(ddp)] (2.05 Å)[6] but similar to those in **3a** (1.95–1.96 Å) and the cationic complex [{(ddp)Ga·thf}$_2$Au][BAr^F] (1.94–1.97 Å).[13] The hydrides could not be located in the solid-state structure. The most striking structural feature of this complex is the parallel arrangement of the GaN_2 planes. Thus, a twist of 90° would be sterically favorable and the fact that the ligands adopt a coplanar arrangement must be explained either electronically or by packing effects. Hence, an overlap of the empty p_z (Ga) orbitals and a filled Pt orbital of suitable symmetry (e.g. p_z) in the square-planar d^8 complex explains this geometry. However, other results in this paper (e.g. the geometrical features of complexes **1**, **2a**, and **2b**, vide supra) suggest this classical π-backbonding, as recently calculated to be relevant for the naked Ga$^+$ ion,[32] to be rather weak.

The molecular structure of the dimeric tetrahydrido complex **9** is also shown in Figure 3. Crystals suitable for X-ray analysis were obtained by recrystallization of the crude product from thf. It crystallizes in the monoclinic space group *P*2$_1$/*n*. The molecular structure shows a coplanar arrangement of the Pt and Ga centers, with the [Ga(ddp)] moiety in a bridging position between the two Pt centers (Pt–Ga distances of 2.46 and 2.48 Å), similar to **5a** and **5b**. The Pt–Pt distance (2.977 Å) is significantly longer than in **3a** (2.614 Å), **5a** (2.634 Å), or the dimeric compound [Pt$_2$(GaCp*)$_5$] (2.58 Å).[28] The Ga–N distances in **9** are 1.967 and 1.960 Å and are therefore quite similar to those in **3a** (1.95–1.96 Å).

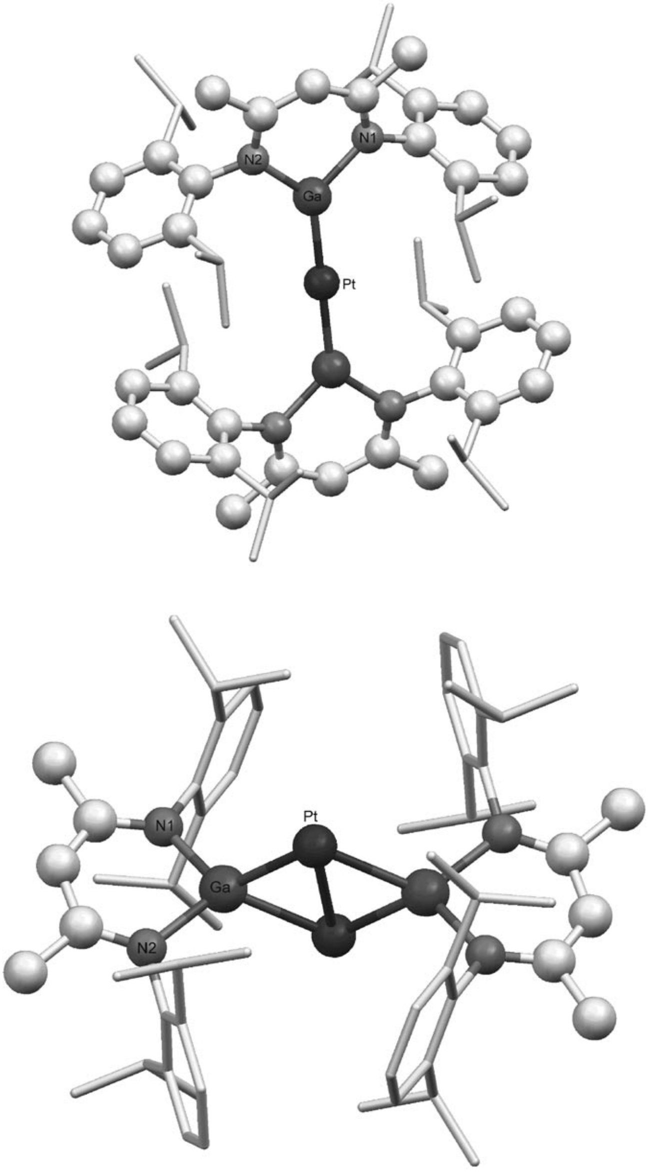

Figure 3. Mercury plot of **7** (top) and **9** (bottom). Hydrogen atoms have been omitted for clarity. Selected bond lengths [Å] and angles [°] for **7**: Pt–Ga 2.3040(15), Ga–N1 1.944(6), Ga–N2 1.960(6); Ga-Pt-Ga* 180.00(5), N1-Ga-N2 93.8(3), N1-Ga-Pt 130.45(19), N2-Ga-Pt 135.3(2). *= symmetry code: $-x+1/2$, $-y+1/2$, $-z$. Selected bond lengths [Å] and angles [°] for **9**: Pt–Ga 2.4618(9), Pt–Ga* 2.4794(10), Pt–Pt* 2.9768(8), Ga–N1 1.961(4), Ga–N2 1.968(5); Pt-Ga-Pt* 74.09(3), Ga-Pt-Ga* 105.91(3), N1-Ga-N2 94.79(19). *= symmetry code: $-x+1$, $-y+2$, $-z+2$.

Crystals of **8** suitable for X-ray analysis were grown by cooling a saturated solution in hexane to −30 °C overnight. The molecular structure is shown in Figure 4 and consists of a Pt center surrounded by two [Ga(ddp)] ligands situated *cis* to each other as well as to an $SiEt_3$ moiety, with the Pt, Ga and Si atoms adopting a coplanar arrangement (angular sum: 360.0°). The hydride ligand could not be located in the solid-state structure. However, the arrangement of the li-

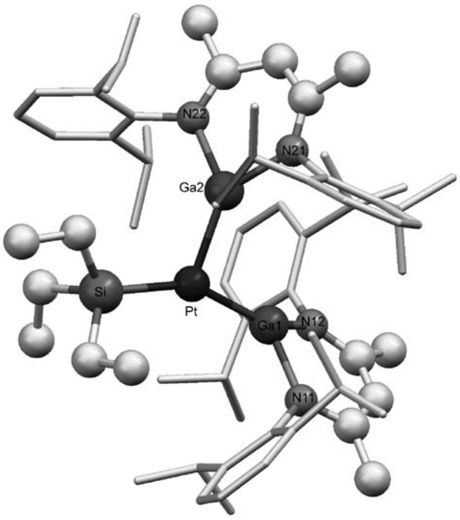

Figure 4. Mercury plot of **8**. Hydrogen atoms have been omitted for clarity. Selected bond distances [Å] and angles [°]: Pt–Ga1 2.3694(9), Pt–Ga2 2.3713(6), Pt–Si 2.3599(12), Ga1–N11 2.005(3), Ga1–N12 1.996(3), Ga2–N21 2.004(3), Ga2–N22 1.993(3); Si-Pt-Ga1 150.09(3), Si-Pt-Ga2 105.75(3), Ga1-Pt-Ga2 104.15(3), N11-Ga1-N12 91.38(11), N21-Ga2-N22 91.41(11).

gands around the platinum center can best be described as a slightly distorted T-shape. Thus, two small angles (Si-Pt-Ga2 105.7° and Ga2-Pt-Ga1 104.1°) and one considerably larger angle (Si-Pt-Ga1 150.1°) create an open coordination site, which suggests that the hydride is located *trans* to Ga2. Considering the high steric demand of the [Ga(ddp)] ligand, the *cis* coordination of the two [Ga(ddp)] moieties is somewhat unusual but consistent with the coordination of the space-consuming $SiEt_3$ ligand.

The Pt–Ga distances are very similar (2.36 and 2.38 Å) and somewhat longer than in **1** (2.34 Å), while the Ga–N distances (1.993–2.005 Å) are in the same range as found for **1**. The Pt–Si bond length (2.360 Å) is quite similar to the Pt–Si bond lengths in *trans*-[Pt(H)(SiH_3)(PCy_3)$_2$] (2.38 Å).[33]

Conclusion

We have shown that the low-valent Group-13 bis-imidinates [Ga(ddp)] and [Al(ddp)] are potent ligands for the reactive, unsaturated d^{10} metal centers Pd^0 and Pt^0. The selective, partial substitution of cod from [Pt(cod)$_2$] by [Ga(ddp)] yields the monomeric complex [Pt(cod){Ga(ddp)}$_2$] (**1**), while [(dvds)Pd{E(ddp)}] (E = Ga (**2a**), Al (**2b**)) can be prepared by addition of [E(ddp)] to [Pd$_2$(dvds)$_3$]. Both **1** and **2a** react readily with strong π-acceptor ligands such as CO or *t*BuNC to give the dimeric cluster compounds [{M[Ga(ddp)]L}$_2$] (M = Pd, Pt; L = CO, *t*BuNC). Based on ^{1}H NMR studies we suggest the formation of [M{Ga(ddp)}$_2$(L)] as intermediates. The observed oxidative addition of H_2 yields the Pt^{II} dihydride species **7** and **9** with **1** as starting compound or a 1:1 mixture of [Pt(cod)$_2$] and [Ga(ddp)]. Accordingly, the first step in the formation of **7** is suggested to be the formation of the *cis* dihydride complex *cis*-[Pt{Ga(ddp)}$_2$(H)$_2$], based on the spectroscopic characterization of this intermediate. Finally, the hydrogenation of a 1:1 mixture of [Pt(cod)$_2$] and [Ga(ddp)] leads to the dimeric cluster compound [{Pt[Ga(ddp)](H)$_2$}$_2$] (**9**). The catalytic hydrogenation of cod in these reactions is a promising finding which may stimulate further studies. The same is true for the apparently nicely reversible oxidative addition of $HSiEt_3$ to **1** to give *cis*-[Pt{Ga(ddp)}$_2$(H)($SiEt_3$)] (**8**), which is quite similar to our report on the chemistry of the [Ni(AlCp*)$_3$] fragment.[16] The observation of H/D exchange with the solvent C_6D_6 again shows the potential of [E(ddp)] ligands to act as ancillary directing ligands similar to NHCs and phosphanes in classical organometallic chemistry. Our experimental findings are well consistent with previous calculations on these classes of compounds and show their strong σ-donor but rather weak π-acceptor properties.[4] The sterically demanding ligands E(ddp) are obviously not only isolobal with, but also electronically similar to, the widely used NHC ligands according to the geometrical features of their solid-state structures, their spectroscopic data, as well as the reactivities of the transition-metal complexes presented in this work.

Experimental Section

All manipulations were carried out under an atmosphere of purified argon using standard Schlenk and glove box techniques. Toluene and hexane were dried using an mBraun Solvent Purification System, and benzene was purified by distillation over chunks of sodium. The final H_2O content in all solvents was checked by Karl–Fischer titration and did not exceed 5 ppm. [Pt(cod)$_2$],[34] [Pd$_2$(dvds)$_3$],[27] [Ga(ddp)],[6] and [Al(ddp)][5] were prepared according to literature methods. Elemental analyses were performed by the Microanalytical Laboratory of the Ruhr-Universität Bochum. NMR spectra were recorded with a Bruker Avance DPX-250 spectrometer (^{1}H: 250.1 MHz; ^{13}C: 62.9 MHz) in C_6D_6 or [D$_8$]THF at 298 K, unless stated otherwise. Chemical shifts are given relative to TMS and were referenced to the solvent resonances as internal standards.

All crystal structures were measured with an Oxford Excalibur 2 diffractometer using Mo$_{K\alpha}$ radiation ($\lambda = 0.71073$ Å). The structures were solved by direct methods using SHELXS-97 and refined against F^2 on all data by full-matrix least-squares with SHELXL-97. The electron density of the oxygen atoms in **3a** adopts a disk-like shape, thus simulating a short C–O distance of 0.911(1) Å. Details of the measurements are given in Tables 1 and 2.

CCDC-616029 (**1**), -616030 (**2a**), -616031 (**2b**), -616032 (**3a**), -616033 (**3b**), -616034 (**5a**), -616035 (**5b**), -616036 (**6**), -616037 (**7**), -616038 (**8**), and -616039 (**9**) contain the supplementary crystallographic data for this paper. These data can be obtained free of charge from The Cambridge Crystallographic Data Centre via www.ccdc.cam.ac.uk/data request/cif.

[(1,3-cod)Pt{Ga(ddp)}$_2$] (1): [Pt(cod)$_2$] (250 mg, 0.62 mmol) and [Ga(ddp)] (629 mg, 1.29 mmol) in hexane (10 mL) were stirred overnight at room temperature. The resulting orange solid was separated from the supernatant solution and redissolved by addition of hexane (10 mL). Cooling the solution to −30 °C overnight yielded orange-red crystals. Yield: 580 mg (74 %). ^{1}H NMR (C_6D_6, 25 °C): $\delta = 7.15$ (br), 4.99 (s, 1H; γ-CH), 3.45–0.84 ppm (br, overlapping signals); ^{13}C NMR (C_6D_6, RT): $\delta = 166.10$ (CN), 164.56 (CN), 144.17 (Ar), 143.72 (Ar), 142.83 (Ar), 127.16 (Ar), 126.87 (Ar), 125.02 (Ar), 124.62 (Ar), 123.38 (Ar), 99.98 (γ-C), 35.18 (coordinated C=C), 35.08 (coordinated C=C), 32.17 (free C=C), 29.90 (*C*H(CH$_3$)$_2$), 29.63 (*C*H(CH$_3$)$_2$), 29.46 (*C*H(CH$_3$)$_2$), 28.52 (*C*-*C* in C_8H_{12}), 28.22 (*C*-*C* in C_8H_{12}), 28.05 (*C*H(CH$_3$)$_2$), 27.44 (*C*H(CH$_3$)$_2$), 25.85 (CH-

Table 1. Crystallographic data for compounds **1**, **2a**, **2b**, **3a**, and **3b**.

	1	**2a**	**2b**	**3a**	**3b**
empirical formula	$C_{66}H_{94}Ga_2N_4Pt$	$C_{43}H_{73}GaN_2OPdSi_2$	$C_{43}H_{73}AlN_2OPdSi_2$	$C_{30}H_{41}GaN_2OPt$	$C_{30}H_{41}GaN_2OPd$
M_r [$g\,mol^{-1}$]	1277.98	866.33	823.59	710.46	621.77
temperature [K]	203(2)	213(2)	105(2)	100(2)	113(2)
wavelength [Å]	0.71073	0.71073	0.71073	0.71073	0.71073
crystal system	monoclinic	triclinic	triclinic	monoclinic	monoclinic
space group	$P2_1/c$	$P\bar{1}$	$P\bar{1}$	$P2_1/n$	$P2_1/n$
a [Å]	15.306(6)	11.682(3)	11.5661(14)	12.889(3)	12.810(4)
b [Å]	13.389(5)	12.509(3)	12.2930(10)	14.932(5)	14.925(4)
c [Å]	33.878(13)	16.301(4)	16.1645(16)	15.851(4)	15.958(5)
α [°]	90.00	82.007(7)	82.306(7)	90.00	90.00
β [°]	99.38(10)1	85.095(6)	85.397(9)	107.21(2)	106.97(3)
γ [°]	90.00	82.934(6)	83.030(8)	90.00	90.00
V [Å^3]	6850(5)	2335.5(10)	2256.0(4)	2914.1(13)	2918.0(16)
Z	4	2	2	4	4
ρ_{calcd} [$g\,cm^{-3}$]	1.239	1.232	1.212	1.619	1.415
μ [mm^{-1}]	2.855	1.044	0.516	5.743	1.563
$F(000)$	2632	916	880	1408	1280
2Θ range [°]	2.38–25.06	2.21–25.05	3.19–27.56	3.27–25.06	2.78–25.08
index ranges	$-18 \leq h \leq 17$,	$-13 \leq h \leq 13$,	$-15 \leq h \leq 15$,	$-15 \leq h \leq 15$,	$-14 \leq h \leq 15$,
	$-15 \leq k \leq 14$,	$-12 \leq k \leq 14$,	$-16 \leq k \leq 11$,	$-17 \leq k \leq 12$,	$-17 \leq k \leq 15$,
	$-40 \leq l \leq 23$	$-16 \leq l \leq 19$	$-21 \leq l \leq 21$	$-18 \leq l \leq 18$	$-17 \leq l \leq 19$
reflections collected	11998	7864	10243	5123	5174
reflections unique	7488	6252	6084	4204	3817
goodness-of-fit on F^2	0.921	1.017	0.854	1.040	0.939
final R indices [$I > 2\sigma(I)$]					
$R1$	0.0565	0.0455	0.0443	0.0605	0.0351
$wR2$	0.1285	0.1128	0.0832	0.1633	0.0751
R indices (all data)					
$R1$	0.0935	0.0594	0.0780	0.0709	0.0525
$wR2$	0.1415	0.1200	0.0919	0.1720	0.0801

Table 2. Crystallographic data for compounds **5a**, **5b**, **7**, **8**, and **9**.

	5a	**5b**	**7**	**8**	**9**
empirical formula	$C_{68}H_{100}Ga_2N_6Pt_2$	$C_{68}H_{100}Ga_2N_6Pd_2$	$C_{58}H_{82}Ga_2N_4Pt$	$C_{67}H_{104}Ga_2N_4PtSi$	$C_{29}H_{41}GaN_2Pt$
M_r [$g\,mol^{-1}$]	1531.16	1351.76	1169.81	1328.16	682.45
temperature [K]	108(2)	113(2)	105(2)	113(2)	108(2)
wavelength [Å]	0.71073	0.71073	0.71073	0.71073	0.71073
crystal system	monoclinic	monoclinic	monoclinic	triclinic	monoclinic
space group	$C2/m$	$C2/m$	$C2/c$	$P\bar{1}$	$P2_1/n$
a [Å]	20.146(4)	20.095(14)	24.215(7)	12.3724(11)	12.763(4)
b [Å]	17.485(4)	17.532(2)	13.36(2)	13.109(2)	12.931(4)
c [Å]	12.357(3)	12.374(6)	18.178(3)	23.075(9)	20.113(6)
α [°]	90.00	90.00	90.00	79.17(2)	90.00
β [°]	121.77(3)	121.79(7)	101.087(19)	75.866(17)	92.89(3)
γ [°]	90.00	90.00	90.00	66.380(11)	90.00
V [Å^3]	3700.7(15)	3705(3)	5770(10)	3308.0(14)	3315.1(17)
Z	2	2	4	2	4
ρ_{calcd} [$g\,cm^{-3}$]	1.374	1.212	1.347	1.333	1.367
μ [mm^{-1}]	4.527	1.235	3.383	2.976	5.043
$F(000)$	1536	1404	2392	1376	1352
2Θ range [°]	3.16–27.56	2.99–25.06	2.99–31.35	3.03–36.90	3.20–27.61
index ranges	$-26 \leq h \leq 26$,	$-21 \leq h \leq 23$,	$-4 \leq h \leq 35$,	$-20 \leq h \leq 14$,	$-14 \leq h \leq 16$,
	$-22 \leq k \leq 22$,	$-20 \leq k \leq 15$,	$-18 \leq k \leq 13$,	$-18 \leq k \leq 21$,	$-16 \leq k \leq 16$,
	$-16 \leq l \leq 14$	$-14 \leq l \leq 14$	$-23 \leq l \leq 9$	$-30 \leq l \leq 33$	$-26 \leq l \leq 24$
reflections collected	4380	3375	5520	22710	7651
reflections unique	3615	2497	2107	13401	7651
goodness-of-fit on F^2	0.985	0.953	0.706	0.829	0.883
final R indices [$I > 2\sigma(I)$]					
$R1$	0.0365	0.0353	0.0530	0.0442	0.0388
$wR2$	0.0887	0.0743	0.0857	0.0738	0.0696
R indices (all data)					
$R1$	0.0457	0.0549	0.1385	0.0792	0.0748
$wR2$	0.0929	0.0795	0.1018	0.0799	0.0770

(*C*H$_3$)$_2$), 25.21 (CH(*C*H$_3$)$_2$), 24.70 (CH(*C*H$_3$)$_2$), 24.42 (CH(*C*H$_3$)$_2$), 23.26 (*C*-*C* in C_8H_{12}), 21.10 (*C*-*C* in C_8H_{12}), 14.56 (C*Me*), 11.88 ppm (C*Me*); elemental analysis calcd (%) for $C_{66}H_{94}Ga_2N_4Pt$: C 62.12, H 7.57, N 4.29; found: C 62.05, H 7.34, N 4.38.

[{(ddp)Ga}Pd(dvds)] (2a): [Pd_2(dvds)$_3$] (583 mg, 0.61 mmol) and [Ga(ddp)] (600 mg, 1.23 mmol) were dissolved in hexane (10 mL) and stirred at room temperature overnight. Traces of black precipitate were removed with a cannula and the solvent removed in vacuo. The crude product was recrystallized from hexane (−30°C overnight) to give yellow crystals. Yield: 780 mg (97%). ^{1}H NMR (C_6D_6, 25°C): δ=7.15 (m, 6H), 5.21 (s, 1H; γ-CH), 3.01 (sept, $J_{\mathrm{H,H}}$=7 Hz, 4H; MeC*H*Me), 2.98–2.59 (m, 6H; dvds), 1.69 (s, 6H; CH_3), 1.22 (d, $J_{\mathrm{H,H}}$=7 Hz, 12H; CH(*Me*)$_2$), 1.10 (d, $J_{\mathrm{H,H}}$=7 Hz, 12H; CH(*Me*)$_2$), 0.44 (s, 6H; Si(*Me*)$_2$), −0.16 ppm (s, 6H; Si(*Me*)$_2$); ^{13}C NMR (C_6D_6, room temp.): δ=166.62 (CN), 142.98 (Ar), 142.57(Ar), 124.67(Ar), 100.33 (γ-C), 60.01(*C*H$_2$CH), 57.59(CH$_2$*C*H), 29.18 (*C*H(CH$_3$)$_2$), 24.86 (CH(*C*H$_3$)$_2$), 24.24 (CH(*C*H$_3$)$_2$), 24.06 (C*Me*), 2.22 (Si*Me*), −0.60 ppm (Si*Me*); elemental analysis calcd (%) for $C_{37}H_{59}GaN_2PdOSi_2$: C 56.71, H 7.57, N 3.60; found: C 56.97, H 7.57, N 3.59.

[{(ddp)Al}Pd(dvds)] (2b): This complex was synthesized analogously to **2a** from [Pd_2(dvds)$_3$] (43 mg, 0.045 mmol) and [Al(ddp)] (100 mg, 0.225 mmol). Yield: 49 mg (74%). ^{1}H NMR (C_6D_6, 25°C): δ=7.15 (m, 6H), 5.21 (s, 1H; γ-CH), 3.02 (sept, $J_{\mathrm{H,H}}$=7 Hz, 4H; C*H*(Me)$_2$), 2.76–2.42 (m, 6H; dvds), 1.61 (s, 6H; CH_3), 1.27 (d, $J_{\mathrm{H,H}}$=7 Hz, 12H; CH(*Me*)$_2$), 1.07 (d, $J_{\mathrm{H,H}}$=7 Hz, 12H; CH(*Me*)$_2$), 0.52 (s, 6H; Si(*Me*)$_2$), −0.20 ppm (s, 6H; Si(*Me*)$_2$); ^{13}C NMR (C_6D_6, RT): δ=168.68 (CN), 143.21 (Ar), 141.26 (Ar), 124.67 (Ar), 100.56 (γ-C), 53.61 (*C*H$_2$CH), 52.94 (CH$_2$*C*H), 31.95 (*C*H(CH$_3$)$_2$), 24.28 (CH(*C*H$_3$)$_2$), 23.98 (CH(*C*H$_3$)$_2$), 23.04 (C*Me*), 2.26 (Si*Me*), −0.76 ppm (Si*Me*); elemental analysis calcd (%) for $C_{37}H_{59}AlN_2PdOSi_2$: C 60.26, H 8.06, N 3.80; found: C 59.86, H 8.14, N 3.98.

[Pt{μ^2-Ga(ddp)}(CO)]$_2$ (3a): Complex **1** (200 mg, 0.157 mmol) was dissolved in hexane (5 mL). CO was bubbled through the solution for approximately 15 minutes and a yellow precipitate was formed. The solvent was removed in vacuo and the resulting solid washed with hexane. Yield: 100 mg (90%). Elemental analysis calcd (%) for $C_{60}H_{82}Ga_2N_4O_2Pt_2$: C 50.72, H 5.82, N 3.94; found: C 50.71, H 5.69, N 4.32.

[Pd{μ^2-Ga(ddp)}(CO)]$_2$ (3b): This complex was prepared analogously to **3a** but from **2a** (150 mg, 0.19 mmol) instead of **1**. Recrystallization from benzene gave yellow, rhombohedral crystals. Yield: 85 mg (74%). ^{1}H NMR (C_6D_6, 25°C): δ=7.15 (m, 6H), 4.95 (s, 1H; γ-CH), 3.28 (sept, $J_{\mathrm{H,H}}$=7 Hz, 4H; C*H*(Me)$_2$), 1.532 (s, 6H; CH_3), 1.16 (d, $J_{\mathrm{H,H}}$=7 Hz, 12H; CH(*Me*)$_2$), 1.13 ppm (d, $J_{\mathrm{H,H}}$=7 Hz, 12H; CH(*Me*)$_2$); ^{13}C NMR (C_6D_6, RT): δ=165.63 (CN), 143.88 (Ar), 142.24 (Ar), 130.41 (Ar), 130.07 (Ar), 129.89 (Ar), 129.49 (Ar), 127.13 (Ar), 124.43 (Ar), 100.58 (γ-C), 29.40 (*C*H(CH$_3$)$_2$), 26.41 (CH(*C*H$_3$)$_2$), 24.84 (CH(*C*H$_3$)$_2$), 23.91 ppm (C*Me*). IR (KBr): ν_{CO}=1957 cm^{-1}; elemental analysis calcd (%) for $C_{60}H_{82}Ga_2N_4O_2Pd_2$: C 57.53, H 6.84, N 4.56; found: C 57.95, H 6.65, N 4.51.

[Pt{Ga(ddp)}$_2$(CO)] (4): [(1,3-cod)Pt{Ga(ddp)}$_2$] (20 mg, 0.0157 mmol) was dissolved in C_6D_6 (0.6 mL) in a J-Young NMR tube. The tube was cooled to −80°C, evacuated, and refilled with CO. ^{1}H NMR (C_6D_6, 25°C): δ=7.15 (m, 6H), 4.94 (s, 2H; γ-CH), 3.09 (sept, $J_{\mathrm{H,H}}$=7 Hz, 8H; C*H*(Me)$_2$), 1.51 (s, 12H; CH_3), 1.23 (d, $J_{\mathrm{H,H}}$=7 Hz, 24H; CH(*Me*)$_2$), 1.14 (d, $J_{\mathrm{H,H}}$=7 Hz, 24H; CH(*Me*)$_2$); ^{13}C NMR (C_6D_6, RT): δ=166.06 (CN), 143.29 (Ar), 142.44 (Ar), 124.64 (Ar), 100.36 (γ-C), 29.31 (*C*H(CH$_3$)$_2$), 25.84 (*C*H(CH$_3$)$_2$), 24.76 (CH(*C*H$_3$)$_2$), 24.44 ppm (C*Me*).

[Pt{μ^2-Ga(ddp)}(*t*BuNC)]$_2$ (5a): Complex **1** (130 mg, 0.102 mmol) was dissolved in thf (5 mL) and carefully layered with hexane (2 mL). *t*BuNC was added to the upper layer to give dark-red/violet crystals at the interface after 15 h at room temperature. Yield: 150 mg (96%). Elemental analysis calcd (%) for $C_{68}H_{100}Ga_2N_4Pt_2$: C 53.34, H 6.58, N 5.49; found: C 53.12, H 6.74, N 6.00.

[Pd{μ^2-Ga(ddp)}(*t*BuNC)]$_2$ (5b): This compound was prepared analogously to **5a** from **2a** (100 mg, 0.13 mmol) and *t*BuNC (11 mg, 0.13 mmol). Yield: 85 mg (96%). Elemental analysis calcd (%) for $C_{68}H_{100}Ga_2N_4Pd_2$: C 60.33, H 7.45, N 6.21; found: C 59.97, H 7.82, N 6.50.

[(ddp)Ga(*t*BuNC)] (6): [Ga(ddp)] (58 mg, 0.12 mmol) was dissolved in hexane (5 mL) at room temperature and an excess of *t*BuNC was added with a syringe. The reaction mixture was heated to 60°C and stirred for 1 h. All volatiles were removed in vacuo and the crude product recrystallized from hexane (−30°C, overnight). Yield 60 mg (89%). ^{1}H NMR (C_6D_6, room temp.): δ=7.15–6.98 (m, 6H), 4.88 (s, 1H; γ-CH), 3.66 (sept, $J_{\mathrm{H,H}}$=7 Hz, 2H; C*H*(Me)$_2$), 3.21 (sept, $J_{\mathrm{H,H}}$=7 Hz, 2H; C*H*(Me)$_2$), 1.56 (s, 6H; CH_3), 1.53 (d, $J_{\mathrm{H,H}}$=7 Hz, 6H; CH(*Me*)$_2$), 1.26 (d, $J_{\mathrm{H,H}}$=7 Hz, 6H; CH(*Me*)$_2$), 1.20 (d, $J_{\mathrm{H,H}}$=7 Hz, 6H; CH(*Me*)$_2$), 0.98 (d, $J_{\mathrm{H,H}}$=7 Hz, 6H; CH(*Me*)$_2$), 0.75 ppm (s, 9H; *t*Bu); ^{13}C NMR (C_6D_6, RT): δ=170.1 (CN), 145.6 (Ar), 142.5 (Ar), 142.0 (Ar), 125.5 (Ar or CN), 123.7 (Ar or CN), 98.0 (γ-CH), 30.7 (CH(*C*H$_3$)$_2$), 29.5 (CH(*C*H$_3$)$_2$), 28.3 (CH(*C*H$_3$)$_2$), 26.1 (CH(*C*H$_3$)$_2$), 24.8 (C*Me*), 23.5 (C*Me*), 23.4 ppm (C*Me*); elemental analysis calcd (%) for $C_{34}H_{50}GaN_3$: C 71.58, H 8.83, N 7.37; found: C 71.35, H 8.95, N 7.02.

[Pt{Ga(ddp)}$_2$(H)$_2$] (7): Complex **1** (155 mg, 0.122 mmol) was dissolved in hexane (5 mL). The reaction vessel was then cooled to −78°C, evacuated, warmed to room temperature, and filled with hydrogen (2 bar). The reaction mixture was stirred for 3 h until a yellow precipitate had formed. The supernatant solution was removed with a cannula and the remaining solid washed with cold hexane and dried in an argon flow. Recrystallization from hexane gave yellow, rhombohedral crystals. Yield: 75 mg (52%). ^{1}H NMR (C_6D_6, 25°C): δ=7.05 (m, 6H), 5.07 (s, 2H; γ-CH), 3.07 (sept, $J_{\mathrm{H,H}}$=7 Hz, 8H; C*H*(Me)$_2$), 1.62 (s, 12H; CH_3), 1.17 (d, $J_{\mathrm{H,H}}$=7 Hz, 24H; CH(*Me*)$_2$), 1.13 (d, $J_{\mathrm{H,H}}$=7 Hz, 24H; CH(*Me*)$_2$), −4.50 ppm (t, $J_{\mathrm{Pt,H}}$=334 Hz; 2H); ^{13}C NMR (C_6D_6, room temp.): δ=166.7 (CN), 143.3 (Ar), 141.1 (Ar), 126.8 (Ar), 123.9 (Ar), 99.2 (γ-C), 28.9 (*C*H(CH$_3$)$_2$), 26.1 (CH(*C*H$_3$)$_2$), 24.3 (CH(*C*H$_3$)$_2$), 23.8 ppm (C*Me*); elemental analysis calcd (%) for $C_{58}H_{84}Ga_2N_4Pt$: C 59.45, H 7.23, N 4.78; found: C 58.64, H 7.58, N 5.00.

[Pt{Ga(ddp)}$_2$(H)(SiEt$_3$)] (8): Complex **1** (250 mg, 0.196 mmol) and $HSiEt_3$ (23 mg, 0.196 mmol) in hexane (5 mL) were stirred at room temperature for 3 h. The solvent was removed in vacuo and the resulting orange solid redissolved in hexane (2 mL). Cooling the solution to −30°C overnight gave orange crystals. Yield: 120 mg (49%). ^{1}H NMR (C_6D_6, RT): δ=7.15 (br. m, arom, 12H), 4.97 (s, 2H; γ-CH), 3.30 (br. sept., $J_{\mathrm{H,H}}$=7 Hz, 4H; *i*Pr-CH), 3.12 (br. sept., $J_{\mathrm{H,H}}$=7 Hz, 4H; *i*Pr-CH), 2.63 (br. sept., $J_{\mathrm{H,H}}$=7 Hz, 4H; *i*Pr-CH), 1.56 (br. s, 6H; CMe), 1.53 (br. s, 6H; CMe), 1.49 (br. d, $J_{\mathrm{H,H}}$=7 Hz, 12H; *i*Pr-*Me*), 1.46 (br. d, $J_{\mathrm{H,H}}$=7 Hz, 12H; *i*Pr-*Me*), 1.33 (br. d, $J_{\mathrm{H,H}}$=7 Hz, 12H; *i*Pr-*Me*), 1.19 (q, $J_{\mathrm{H,H}}$=8 Hz, 6H; C*H$_2$*CH$_3$), 1.11 (br. d, $J_{\mathrm{H,H}}$=7 Hz, 12H; *i*Pr-*Me*), 0.93 (t, $J_{\mathrm{H,H}}$=8 Hz, 9H; CH$_2$C*H$_3$*), −5.63 ppm (s, $J_{\mathrm{Pt,H}}$=530 Hz, 1H; Pt-H); ^{1}H NMR (C_6D_6, 70°C): δ=7.15 (br., arom, 12H), 5.04 (s, 2H; γ-C*H*), 3.16 (br. sept., 8H; *i*Pr-CH), 1.55 (br. s, 12H; C*Me*), 1.24 (q, 6H; C*H$_2$*CH$_3$), 1.15 (br., 48H; *i*Pr-*Me*), 0.86 (t, 9H; CH$_2$C*H$_3$*); ^{13}C NMR (C_6D_6, RT): δ=170.1 (CN), 166.9 (CN), 166.8 (CN), 144.6 (Ar), 144.0 (Ar), 143.6 (Ar), 142.5 (Ar), 129.0 (Ar), 128.6 (Ar), 127.8 (Ar), 124.5 (Ar), 100.3 (γ-C), 31.90 (*C*H(CH$_3$)$_2$), 29.4–28.2 (broad and overlapping signals, not assignable), 25.0–24.3 (broad and overlapping signals, not assignable), 23.0 (C*Me*), 15.9 (C*Me*), 14.3 (CH$_2$*C*H$_3$), 11.1 ppm (*C*H$_2$CH$_3$); elemental analysis calcd (%) for $C_{64}H_{98}Ga_2N_4Pt$: C 59.77, H 7.68, N 4.36; found: C 59.83, H 8.03, N 4.82.

[Pt{μ^2-Ga(ddp)}(H)$_2$]$_2$ (9): [Pt(cod)$_2$] (100 mg, 0.24 mmol) and [Ga(ddp)] (118 mg, 0.24 mmol) were dissolved in thf (5 mL). The reaction vessel was then cooled to −78°C, evacuated, warmed to room temperature, and filled with hydrogen (2 bar). After the reaction mixture had been stirred for 6 h, a yellow precipitate had formed. The supernatant solution was removed with a cannula and the crude product recrystallized from thf and dried in an argon flow. Yield: 62 mg (38%). ^{1}H NMR (C_6D_6, 25°C): δ=7.01–6.82 (m, 6H), 4.89 (s, 1H; γ-CH), 3.35 (sept, $J_{\mathrm{H,H}}$=7 Hz, 4H; C*H*(Me)$_2$), 1.47 (s, 6H; CH_3), 1.11 (d, $J_{\mathrm{H,H}}$=7 Hz, 12H; CH(*Me*)$_2$), 0.80 (d, $J_{\mathrm{H,H}}$=7 Hz, 12H; CH(*Me*)$_2$), −4.06 ppm (br, 2H; Pt-H); ^{13}C NMR (C_6D_6, RT): δ=168.7 (CN), 144.2 (Ar), 140.9 (Ar), 127.1 (Ar), 124.3 (Ar), 97.7 (γ-C), 28.6 (*C*H(CH$_3$)$_2$), 25.8 (CH(*C*H$_3$)$_2$), 25.4 (CH(*C*H$_3$)$_2$), 23.8 ppm (C*Me*); elemental analysis calcd (%) for $C_{58}H_{86}Ga_2N_4Pt_2$: C 50.89, H 6.33, N 4.09; found: C 50.40, H 6.17, N 4.05.

---

[1] E. O. Fischer, A. Maasböl, *Angew. Chem.* **1964**, *76*, 645; *Angew. Chem. Int. Ed. Engl.* **1964**, *3*, 580.
[2] A. C. Filippou, H. Rohde, G. Schnakenburg, *Angew. Chem.* **2004**, *116*, 2293; *Angew. Chem. Int. Ed.* **2004**, *43*, 2243.
[3] W. A. Herrmann, *Angew. Chem.* **2002**, *114*, 1342; *Angew. Chem. Int. Ed.* **2002**, *41*, 1290.
[4] R. J. Baker, C. Jones, *Coord. Chem. Rev.* **2005**, *249*, 1857.
[5] C. Chui, H. Roesky, H.-G. Schmidt, M. Noltemeyer, H. Hao, F. Cimpoesu, *Angew. Chem.* **2000**, *112*, 4444; *Angew. Chem. Int. Ed.* **2000**, *39*, 4274.
[6] N. J. Hardman, B. E. Eichler, P. P. Power, *Chem. Commun.* **2000**, 1991.
[7] M. S. Hill, P. B. Hitchcock, *Chem. Commun.* **2004**, 1818.
[8] M. S. Hill, P. B. Hitchcock, R. Pongtavornpinyo, *Dalton Trans.* **2005**, 273.
[9] E. S. Schmidt, A. Jokisch, H. Schmidbaur, *J. Am. Chem. Soc.* **1999**, *121*, 9758.
[10] C. Jones, P. C. Junk, J. A. Platts, A. Stasch, *J. Am. Chem. Soc.* **2006**, *128*, 2206.
[11] N. Hardman, R. J. Wright, A. D. Philips, P. Power, *J. Am. Chem. Soc.* **2003**, *125*, 2667.
[12] A. Kempter, C. Gemel, R. A. Fischer, *Inorg. Chem.* **2005**, *44*, 163.
[13] A. Kempter, C. Gemel, N. J. Hardman, R. A. Fischer, *Inorg. Chem.* **2006**, *45*, 3133.
[14] A. Kempter, C. Gemel, R. A. Fischer, *Chem. Commun.* **2006**, 1551.
[15] C. Gemel, T. Steinke, M. Cokoja, A. Kempter, R. A. Fischer, *Eur. J. Inorg. Chem.* **2004**, 4161.
[16] T. Steinke, C. Gemel, M. Cokoja, M. Winter, R. A. Fischer, *Angew. Chem.* **2004**, *116*, 2349; *Angew. Chem. Int. Ed.* **2004**, *42*, 2247.
[17] T. Steinke, M. Cokoja, C. Gemel, A. Kempter, A. Krapp, G. Frenking, U. Zenneck, R. A. Fischer, *Angew. Chem.* **2005**, *117*, 3003; *Angew. Chem. Int. Ed.* **2005**, *44*, 2943.
[18] T. Cadenbach, C. Gemel, R. Schmid, S. Block, R. A. Fischer, *Dalton Trans.* **2004**, 3171.
[19] T. Cadenbach, C. Gemel, R. Schmid, R. A. Fischer, *J. Am. Chem. Soc.* **2005**, *127*, 17068.
[20] B. Buchin, C. Gemel, T. Cadenbach, R. A. Fischer, *Inorg. Chem.* **2006**, *45*, 1789.
[21] M. Cokoja, C. Gemel, T. Steinke, F. Schroeder, R. A. Fischer, *Dalton Trans.* **2005**, 44.
[22] T. Steinke, C. Gemel, M. Cokoja, M. Winter, R. A. Fischer, *Chem. Commun.* **2003**, 1066.
[23] T. Steinke, C. Gemel, M. Cokoja, R. A. Fischer, *Dalton Trans.* **2005**, 55.
[24] B. Buchin, C. Gemel, T. Cadenbach, R. A. Fischer, *Z. Anorg. Allg. Chem.* **2005**, *631*, 2756.
[25] J. P. Collman, L. S. Hegedus, J. R. Norton, R. G. Finke, *Principles and Applications of Organotransition Metal Chemistry*, University Science Books, **1987**.
[26] R. Benn, P. Betz, R. Goddard, P. W. Jolly, N. Kokel, C. Koger, I. Topalovic, *Z. Naturforsch. Teil B* **1991**, *46*, 1395.
[27] J. Krause, G. Cestaric, K.-J. Haak, K. Seevogel, W. Storm, K.-R. Pörschke, *J. Am. Chem. Soc.* **1999**, *121*, 9807.
[28] T. Steinke, C. Gemel, M. Winter, R. A. Fischer, *Chem. Eur. J.* **2005**, *11*, 1636.
[29] G. Booth, J. Chatt, P. Chini, *Chem. Commun. (London)* **1965**, 639.
[30] M. Green, J. A. Howard, J. L. Spencer, F. G. A. Stone, *J. Chem. Soc. Chem. Commun.* **1975**, 3.
[31] A. E. Shilov, G. B. Shulpin, *Chem. Rev.* **1997**, *97*, 2879.
[32] B. Buchin, C. Gemel, T. Cadenbach, I. Fernandez, G. Frenking, R. A. Fischer, *Angew. Chem.* **2006**, *118*, 5331; *Angew. Chem. Int. Ed.* **2006**, *45*, 5207.
[33] E. A. V. Ebsworth, V. M. Marganian, F. J. S. Reed, R. O. Gould, *J. Chem. Soc. Dalton Trans.* **1978**, 1167.
[34] M. Green, J. A. K. Howard, J. L. Spencer, F. G. A. Stone, *J. Chem. Soc. Dalton Trans.* **1977**, 271.

Received: July 28, 2006